

APPLICATION OF FT-IR SPECTROSCOPY TO STUDY HYDROCARBON REACTION CHEMISTRY

Peter R. Solomon, David G. Hamblen, Robert M. Carangelo,
James R. Markham and Michele R. Chaffee

Advanced Fuel Research, Inc., 87 Church Street, East Hartford, CT 06108, USA

Fourier Transform Infrared Spectroscopy (FT-IR) is one of the most versatile analytical techniques available for the study of fossil fuel structure and reaction chemistry. Among its advantages are: (i) its ability to study feedstocks and reaction products as solids, liquids and gases, since almost all have characteristic absorptions in the infrared; (ii) its sensitivity, allowing the study of highly absorbing materials such as coal and char and the use of difficult techniques such as photoacoustic or diffuse reflectance spectroscopy; (iii) its speed (instruments commercially available can obtain a complete spectrum every 20 milliseconds) allowing the possibility of following chemical reactions on-line; (iv) its inherent rejection of stray radiation, allowing transmission measurements at elevated temperatures to be made in-situ; (v) its ability to measure emission spectra to determine temperature as well as chemical changes of reactants at elevated temperature.

Because of these advantages, FT-IR spectroscopy has achieved increasing use in fuel science. This paper will review some of its applications. Recent progress has been made in the use of FT-IR for the quantitative determination of hydrogen functional groups in solid hydrocarbons. Developments in this area are important since uncertainties in the hydrogen distribution have hindered investigations of coal structure. The paper will discuss the present convergence being obtained in the determination of aliphatic hydrogen and the uncertainties remaining in the determination of aromatic hydrogen. A second area to be considered will be the application of the functional group determination to the study of coal pyrolysis. The paper will consider the changes in the functional group composition of coal during primary pyrolysis and its relationship to the pyrolysis products which are formed. Finally, recently developed methods employing both emission and transmission spectroscopy will be considered to monitor, in-situ, the coal particle temperature and chemical changes which occur during pyrolysis.

DETERMINATION OF AROMATIC AND ALIPHATIC HYDROGEN IN COAL

While several techniques are available for obtaining infrared spectra of coal, only the KBr pellet technique has been pursued extensively for quantitative analysis. Methods for quantitative preparation of samples have been described in a number of publications (1-7) and it appears that with a representative sample of coal and care in sample preparation, spectra can be repeated with less than 5% variation. Typical KBr pellet spectra for two bituminous coals and a lignite are illustrated in Fig. 1. They have peaks due to their functional groups and mineral components which are identified in the figure. In general, all coals have these absorption bands and the major variation with rank is in their relative magnitude. There are three features of the KBr spectra whose interpretation has been controversial. The first is the large peak at 1600 wavenumbers, which evidence now suggests is an aromatic ring stretch whose intensity is greatly enhanced by the presence of hydroxyl groups on the ring and nitrogen in the ring (2-4,6). The second is the sloping baseline which has generally been attributed to scattering (rather than absorption) of the transmitted radiation by the particles of coal in the KBr pellet. A straight line correction has sometimes been used to obtain a spectrum more "representative" of the absorption. Figure 2 compares a baseline corrected spectrum of coal (a) in Fig. 1. to a spectrum of the same coal obtained by photoacoustic absorption spectroscopy (PAS) (8,9). The PAS technique which is sensitive only to the absorption of energy does not have a sloping baseline and is quite similar in appearance to the baseline-corrected KBr pellet spectrum. The baseline correction appears to be accurate for coals and chars

up to about 90 percent carbon. At high carbon concentrations, a broad sloping absorption is also present. Comparison of the two spectra suggest some distortion of the aliphatic band in the KBr pellet spectrum may occur due to the Christiansen effect. This distortion could influence measurements of the aromatic hydrogen if the 3100 wavenumber band is used. PAS spectra also appear to exaggerate the mineral peaks. A third controversial feature is the hydroxyl band. Is it really as broad as it appears (due to hydrogen bonding) and can the band associated with water incorporated during the pellet preparation be eliminated by drying the pellet? Results of Ref. 1 suggest that drying removes almost all of the water and good results have been obtained using the optical density at 3200 wavenumbers to determine the hydroxyl content. Comparison of the dry KBr pellet spectrum with the PAS spectrum in Fig. 2. suggests that the broad absorption peak of the hydroxyl groups in the dried pellet is real.

To obtain aromatic and aliphatic hydrogen concentrations, $H(ar)$ and $H(al)$, it is necessary to integrate the areas $A(ar)$ and $A(al)$ under the appropriate peaks (spectra are normalized to 1 mg per square cm) and divide by appropriate integral absorptivities $a(ar)$ and $a(al)$ (in abs. units x wavenumbers/mg/cm²) to relate the areas to the hydrogen concentrations. The former task has been automated by employing a synthesis routine which uses a set of preselected peaks whose position and width are held fixed and whose amplitude is varied to reproduce the experimental spectrum (2-4). The technique has the advantage that integrated areas will be obtained in a consistent manner for all samples. Excellent fits have been obtained for hundreds of coal samples using one set of 45 Gaussian peaks (2). To obtain the absorptivities for coal samples, a method was derived (2-4) in which $H(al) = A(al)/a(al)$ and $H(ar) = A(ar)/a(ar)$ was equated to the total hydrogen, H , minus the hydroxyl hydrogen, $H(OH)$ and rearranged to yield the following equation,

$$\frac{1}{a(al)} \left[\frac{A(al)}{H - H(OH)} \right] = 1 - \frac{1}{a(ar)} \left[\frac{A(ar)}{H - H(OH)} \right] \quad (1)$$

If the absorptivities are independent of coal composition, than the two unknowns, $a(ar)$ and $a(al)$ can be determined from $A(al)$, $A(ar)$, H and $H(OH)$ for two samples. $H(OH)$ can be determined chemically or by FT-IR (1,5). $A(al)$ is usually obtained from the set of peaks near 2900 wavenumbers which are strong and do not have any interfering peaks nearby. $A(ar)$ can be obtained from the peaks near 800 wavenumbers which are strong but have interference from mineral peaks (which must be subtracted) and long methylene chains (which are weak and can be subtracted) or from the peak near 3100 wavenumbers which are weak and have interference from the aliphatic and hydroxyl bands. The problem of determining the area for the 3100 wavenumber peak is substantial for low rank coals as will be discussed below.

In practice, coals do not have different enough ratios of $H(al)$ and $H(ar)$ to determine accurately the absorptivities from two samples, so large numbers of coals are used to define a straight line by plotting the two terms in brackets. But, even this method is not accurate because the coals tend to be tightly clustered. To alleviate this problem, coal derived chars and tars, which have related chemical structures were also included to provide a wider range of aliphatic to aromatic ratios (2-4). This will work only if the absorptivities for these additional samples are the same as for coals. A set of chars produced by heating a bituminous coal at 30°C/sec to different final temperatures is illustrated in Fig. 3. As can be seen $A(ar)/A(al)$ increases continuously with pyrolysis temperature. The chars produced above 600°C have little aliphatic hydrogen and thus provide an excellent sample for determining $a(ar)$. Using the 800 wavenumber region for $A(ar)$, the bracketed terms in Eq. 1 are plotted in Fig. 4 with some additional chars and tars from a Pittsburgh Seam coal of similar carbon content. The chars form a regular series along a straight line with intercepts at $a(ar) = 684$ and $a(al) = 744$. The results are in excellent agreement with previously derived values of 686 and 746 for all bituminous coals, chars and tars (2). Model compounds were also examined to provide guidance in the possible absorptivity values (2-4). The $a(ar)$ value is 11% lower than the average value of $a(ar) = 768$ for 25 model compounds containing C and H only. The same model compounds give an average value of

$a(\text{ar}) = 220$ for the 3100 wavenumber band. This corresponds to $\epsilon(\text{ar}) = .60$ in good agreement with the value derived in Refs. 7 and 10.

Using these absorptivities, values of $H(\text{ar})$ and $H(\text{al})$ have been derived for a set of bituminous coals from the Exxon premium sample collection. The results are plotted as a function of rank in Fig. 5a. The values of $H(\text{ar})$ lie in a narrow band which shows a smooth variation with rank. Values of $H(\text{al})$ are more scattered. The scatter in the data appear to reflect real variations in $H(\text{al})$, since $H(\text{al}) + H(\text{ar})$ is in good agreement with $H - H(\text{OH})$ as shown in Fig. 6a. The data form a band with a random variation of $\pm 10\%$. The slight slope in Fig. 6a suggests a variation of the absorptivity with carbon concentration.

The problem of obtaining absorptivities using coals alone (i.e., defining a line through data points clustered in a small region) was recently discussed extensively by researchers at Penn State University (7,10). They used an error minimization procedure (equivalent to the graphical method discussed above) to evaluate the absorptivities for a group of coals and lignites. The 3100 wavenumber region was chosen for $H(\text{ar})$ instead of the 800 wavenumber region. The same method was used on pyridine extracts (7) and it was determined that the absorptivities match reasonably with absorptivities derived from proton nmr. The absorptivity value derived for $a(\text{al})$ was 665, 11% lower than our value of 745. Note the conversion factor $\epsilon(\text{al}) = .20$ in Ref. (10) is the reciprocal of $a(\text{al})$ multiplied by 100 (weight fraction to weight %) and by 1.33 (mg per pellet to mg/cm^2). The results are shown in Fig. 5b. The $H(\text{al})$ values are about 10% higher than ours and are in agreement with the differences in $a(\text{al})$. The 10% extra hydrogen in the $H(\text{al})$ values must be made up in the $H(\text{ar})$ values which are up to 30% to 50% lower than our values at low carbon concentration. A comparison of $H(\text{al}) + H(\text{ar})$ to $H - H(\text{OH})$ is made in Fig. 6b. The random variation is similar to our results ($\pm 12\%$ vs. $\pm 10\%$) but the dependence on carbon concentration is greater. While Reisser et al. (10) have attributed all the discrepancies between $H(\text{al}) + H(\text{ar})$ derived by FT-IR and $H - H(\text{OH})$ derived by elemental analysis and FT-IR to random errors in KBr pellet sample preparation, some of the variation is clearly a systematic rank dependence caused by variations in the absorptivities with rank. This variation was observed in our earlier work and we derived separate absorptivity values for lignites and subbituminous coals (2). The rank variation in the absorptivities using the 3100 wavenumber region appear to be greater than what we have obtained using the 800 wavenumber region. This observation will be discussed below. We believe that the values of $H(\text{ar})$ reported originally (3) were too high because of the influence of the rank variation when using rank independent absorptivities.

Considering the above results, how accurate is the FT-IR method for determining hydrogen functional group concentrations? Both sets of data derived by FT-IR (Figs. 5a and 5b) produce similar values of $H(\text{al})$. Values of $H(\text{ar})$ are in reasonably narrow bands which agree above 85% carbon. The method in its current state of development (using rank independent absorptivities) can, therefore, determine $H(\text{al})$ to $\pm 10\%$ and relative trends for $H(\text{ar})$. The FT-IR technique appears capable of providing accurate absolute values for the hydrogen functional group distribution provided the proper absorptivity can be determined for $H(\text{ar})$ below 85% carbon. As guidance in determining the proper absorptivities, data for $H(\text{ar})$ in coal derived by dipolar dephasing (11) are presented in Fig. 5c and data for pyridine extracts (12,13), vacuum distillates (14) and coals (13) obtained by proton nmr and IR are presented in Fig. 5d. Among these data for $H(\text{ar})$ the dipolar dephasing data (Fig. 5c) are the highest. The data from this work (Fig. 5a) are similar to the data on coal like materials (Fig. 5d) and are within the range of the dipolar dephasing data. The data of Reisser et al. (10), (Fig. 5b) are the lowest and appear outside the range of the dipolar dephasing data.

Another comparison is made in Table I using the average values determined for the ratios of $H(\text{ar})$ to $H(\text{al})$ in the range of 80-85% carbon (10-16). The value of 0.35, determined by Reisser et al., (10) is 24% lower than the cumulative average of 0.46. The value of 0.52 from the present results is 13% too high. The value of 0.2 originally determined by Brown (15) is too low and the value of 0.70 determined by

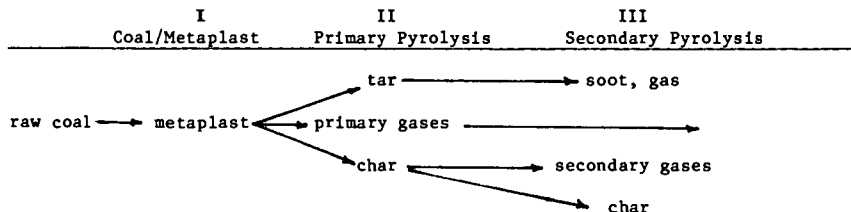
Wilson et al. (11) using dipolar dephasing appears too high.

Some of the discrepancy in the FT-IR values may be due to the choice by the Penn State group (7,10) of the 3100 wavenumber band for H(ar). This band appears to shrink more rapidly with decreasing rank than do the 800 wavenumber bands. A comparison is made in Fig. 7 between these two regions for a lignite, its tar and its char. These samples are low in mineral content. The spectra are presented without baseline or mineral corrections. While the coal shows a distinct band near 800 wavenumbers it is very difficult to distinguish a band at 3100 wavenumbers. The tar and char produced in pyrolysis show large peaks at 800 wavenumbers but only the char has a clearly defined peak at 3100 wavenumbers. The amplitude at 3100 wavenumbers is either weakened or partially hidden by the presence of the hydroxyl band. The ratio of areas of the 3100 to 800 wavenumber bands for the Exxon coals are plotted in Fig. 8a. The ratio goes to zero with increasing rank. A similar effect is observed for model compounds in Fig. 8b. The stretch region appears more sensitive to the oxygen concentration than the wag. For example, a(ar) goes from 220 (25 model compounds without oxygen) to an average value of 122 (8 model compounds with an average of 11% oxygen). For the same model compounds a(ar) for the 800 wavenumber region goes from 768 (no oxygen) to 889 (with oxygen). While this ratio depends on the way the bands are fit (i.e. integration limits and baseline) it is very difficult to avoid very small areas in the 3100 wavenumber region for low rank coals.

The decreasing 3100 wavenumber band intensities for low rank coals would explain the low values of H(ar) in Fig. 5b and the slope in Fig. 6b. Resolution of this issue and improved accuracy in the technique requires the following advances: i) an agreed upon procedure for obtaining peak areas, ii) use of rank dependent absorptivities, iii) a premium set of reproducible samples of coals, vacuum distillates and pyridine extracts for round robin tests at different laboratories using FT-IR, proton nmr and C¹³ nmr with dipolar dephasing. Even with its limitations, the present technique appears to be the best routine method to obtain hydrogen functional group concentrations.

THE VARIATIONS IN FUNCTIONAL GROUP COMPOSITION DURING COAL PYROLYSIS

An application of the analysis method described above was made in the study of coal pyrolysis where the evolution of pyrolysis products may be related to the chemical changes occurring in the coal as determined by FT-IR spectroscopy. Pyrolysis has been described in terms of the following stages:



During, stage I the coal may undergo some bond breaking reactions and reduction of hydrogen bonding which may lead to melting. Some light species which exist as guest molecules or are formed by the breaking of very weak bonds are released. During stage II, further bond breaking occurs leading to evolution of tar and gases and the formation of char. During stage III the products can continue to react. The char can evolve secondary gases, mainly CO and H₂ while undergoing ring condensations. The tars can crack to form soot, coke and gases and the gases can crack to form lighter gases and soot.

To demonstrate the relationship between the "extent of pyrolysis" and the functional group composition, we consider an experiment in which samples of a bituminous coal were heated at a constant rate of 30°C/min starting at 150°C and ending at a series of

temperatures between 350 and 950°C. Slow heating is useful in separating the stages of pyrolysis, which can overlap in rapid heating experiments. Figure 3 shows the infrared spectra obtained for the product chars (at several temperatures) by quantitative FT-IR spectroscopy. There are substantial changes in the spectra as the peak pyrolysis temperature is increased. To relate these changes to the stages of pyrolysis, the functional group compositions from these spectra are compared in Fig. 9 to the weight loss and evolution of tar and gases measured during the experiment.

Substantial changes occur during the primary pyrolysis, stage II. Figure 9a compares the weight loss with the rate of tar evolution. The maximum rate of weight loss at 470°C compares with the maximum rate of tar evolution. Figure 9b shows the rate of aliphatic gas evolution compared to the loss of aliphatic hydrogen, H(al), in the char. There is also an increase in H(ar), Fig. 9e, which occurs as the tar picks up hydrogen from hydroaromatic rings, converting them to aromatic sites. The loss of tar, aliphatic gases and H(ar) are closely coupled events which dominate the primary pyrolysis. The loss of H(al) indicates the end of stage II. The loss of H(al) also signals the loss of plasticity and swelling as described in (17).

At 30°C/min heating rate, secondary pyrolysis, stage III, began above 550°C. Figure 9c compares the evolution of methane with the concentration of methyl groups in the char. The methyl group concentration first increases during primary pyrolysis (due to bond breaking and stabilization) and then decreases as methane is formed. The events occurring during the later parts of stage III include the elimination of ether linkages coupled with the evolution of CO (Fig. 9d) and the elimination of aromatic hydrogen, H(ar), (Fig. 9e) which occurs during ring condensation coupled with evolution of hydrogen gas (not measured in this experiment). Since ring condensations also eliminate active sites for oxygen attack, H(al) should be a good parameter to correlate with intrinsic char reactivity. Figure 9f shows the evolution of CO₂ and H₂O. The evolution of water appears to correlate with the increase in the ether oxygen suggesting that two hydroxyls may combine to form a water and an ether link.

For these experiments, the changes in the functional group composition as determined by FT-IR provide a good chemical description of the pyrolysis stages which are in turn correlated with the evolved products. It has been demonstrated that this relationship between the pyrolysis events and the functional group composition is quite general, being independent of coal rank and temperature (3,17-20). The sequence of functional group changes is the same in high heating rate experiments as for the slow heating case and corresponds in the same way to the pyrolysis events. FT-IR spectra provide a good method to determine the "extent of pyrolysis".

IN-SITU MONITORING OF COAL TEMPERATURE AND SPECTRAL EMITTANCE

As a final example of the FT-IR's versatility, we consider its application in the on-line, in-situ monitoring of coal conversion. In this application the sample volume is in the reacting stream rather than in a KBr pellet. Both emission and transmission measurements are made to provide data on the coal's temperature and spectral emittance (which is related to its chemical composition). As described in a previous publication (21), the transmittance measurement is used to determine the total emitting surface of the coal particles so that a normalized emission, (emission/(1-transmittance)) can be compared in both shape and amplitude to a theoretical black-body. In the work described below, the coal flow rate was monitored to insure that both measurements be made under the same conditions. Also, the emission from several phases (tar in particular) and diffraction effect required additional care in the computation of the normalized emission. Compared to other techniques for measuring temperature the FT-IR normalized emission measurement has the following advantages: 1) A complete spectrum is obtained, not just two or three colors; 2) Measurements are made in the infrared where the emission is strongest and where measurements of emission and optical properties are relevant to practical conversion processes; 3) Measurements are possible with mixed phase (particles, soot and gas); 4) For grey-bodies, the measurement of normalized emittance allows the use of the spectral shape to obtain temperature and the

amplitude, to obtain emissivity; 5) Measurements are fast. A complete spectrum can be obtained in 20 milliseconds using a commercial FT-IR. With this speed, tomographic techniques to obtain point measurements may be practical; 6) Determination of temperature distributions are possible; 7) The technique is applicable to measurements in process equipment.

The spectra which we consider were obtained for pyrolysis measurements made in a tube reactor described in another paper presented at this meeting (22) and combustion measurements made in an entrained flow reactor (17). Both reactors allow optical access to the high temperature products. For these experiments, the FT-IR measurement can provide a direct measurement of the coal particle temperature. The technique has been validated by making measurements under conditions where the particle temperatures are known. A simple case is illustrated in Fig. 10a. For this case, sufficient time was allowed for the coal to reach the asymptotic tube temperature of 935°C (1208 K) and for primary pyrolysis to have occurred. The normalized emission spectrum is in good agreement with a theoretical black-body at 1190 K with an amplitude corresponding to an emissivity of 0.9. The measured temperature is in excellent agreement with the tube temperature, as a 10°C drop in temperature is expected between the end of the tube, and the measuring point at 0.75 cm below the end.

The measurement of temperature before and during pyrolysis is not as simple, since for the size of coal particles used here, only specific bands (corresponding to the absorbing bands in coal) provide sufficient absorbance for the spectral emittance to reach 0.9. Then, only these regions can be used to compare to the black-body. Examples for a 200 x 325 mesh fraction of a Montana Lignite injected at 3 grams/min into the tube reactor at 800°C (1173 K) with a cold helium velocity of 4 m/sec are presented in Figs. 10b and 10c. The same coal with a cold velocity of 28 m/sec is shown in Fig. 10d. The spectrum is noisier due to the lower density of coal at the higher velocity, but has a shape similar to Fig. 10b where the coal is at a comparable temperature. The spectra are decidedly non-black or non-grey. Measurements show that the particle's emissivity is size, rank and temperature dependent. The result can be understood by remembering that a particle's emittance is related to its absorbance. Only the region between 1000 and 1600 wavenumbers has sufficient absorbance to fully attenuate the incident light over the particle thickness. It is only in this region that the normalized emission can be compared to the black-body. The aliphatic and hydroxyl bands are questionable.

Figures 10b to 10d contain the best fit grey-body curve ($\epsilon = 0.9$) in the 1000 to 1600 wavenumber region and a grey-body curve ($\epsilon = 0.9$) corresponding to the thermocouple measurement at the FT-IR focus. The grey-body curves are fit, excluding the region around 1500 wavenumbers where there is interference from water. The differences between the FT-IR and thermocouple measurements were 30°C, 40°C, and -13°C for measurements at 853 K, 953 K, and 913 K, respectively. The three cases are for transit distances of 10, 30 and 50 cm in the tube reactor. The spectra change with particle temperature and with changes in composition as ring condensation (which takes place during pyrolysis) makes the char more graphitic. The emission spectrum approaches a grey-body like Fig. 10a, only after sufficient time at elevated temperature (after primary pyrolysis is complete). The spectrum of Fig. 10c is almost a grey-body ($\epsilon = 0.9$). The spectrum for the same coal at 935°C, Fig. 10a, is even closer. To determine the change under even more severe pyrolysis conditions, chars of the same coal were prepared at 1300°C and then injected into the tube reactor at 800°C. The spectrum in Fig. 10e shows a grey-body with an emissivity of $\epsilon = 0.70$, close to that expected for graphite.

The spectral emittance is also particle size dependent. Figure 10f shows a spectrum for a -400 mesh fraction of the same lignite. Except for the 1200 to 1600 wavenumber region, the spectral emittance is much lower than 0.9. As pyrolysis proceeded and particle mass was lost, the spectral emittance decreased even in the 1200 to 1600 region. These data show that raw coal of a size used for pulverized coal combustion does not have anywhere near the 90% absorption of radiation which is usually assumed in

calculating the particle heating rates. The average spectral emittance in the mid IR (where furnace radiation is a maximum) is about 0.5 for the 200 x 325 mesh fraction and 0.2 for the -400 mesh fraction.

Figure 10g shows that temperature was determined as low as 300°C. Figures 10h and 10i show temperature determinations during combustion. Under identical conditions, the lignite, at 1650 K is much more reactive than the bituminous coal at 1350 K. The particles spectral emittance have fallen to about 0.70 in agreement with the results of Fig. 10e.

ACKNOWLEDGMENT

The support of the Morgantown Energy Technology Center is gratefully acknowledged for the work on coal pyrolysis and on FT-IR emission/transmission spectroscopy. We wish to thank Dr. John McClelland of Ames Laboratory who obtained the photoacoustic spectrum in Fig. 2 and Richard Neavel, at the Exxon Corporation, for permitting the use of data on the Exxon samples.

REFERENCES

1. Solomon, P.R. and Carangelo, R.M., *Fuel*, 61, 663, (1982).
2. Solomon, P.R., Hamblen, D.G., and Carangelo, R.M., "Applications of Fourier Transform IR Spectroscopy in Fuel Science", ACS Symposium Series 205, pg. 77, (1982).
3. Solomon, P.R., *Advances in Chemistry Series*, Vol. 192, "Coal Structure", 95, (1981).
4. Solomon, P.R. and Carangelo, R.M., "Characterization of Wyoming Subbituminous Coals and Liquefaction Products by Fourier Transform Infrared Spectrometry", EPRI Final Report, Project No. 1604-2, (1981).
5. Kuehn, D.W., Snyder R.W., Davis, A., and Painter, P.C., *Fuel*, 61, 682, (1982).
6. Painter, P.C., Starsinic, M., Squires, E., and Davis, A.A., *Fuel*, 62, 742, (1983).
7. Sobkowiak, M., Reisser, E., Given, R., and Painter, P., *Fuel*, 63, 1245, (1984).
8. McClelland, J.F., *Anal. Chem.*, 55, 89A, (1983).
9. Vidrine, D.W., *Fourier Transform Infrared Spectroscopy*, 3, 125, (1982).
10. Riesser, B., Starsinic, M., Squires, E., Davis, A., and Painter, P.C., *Fuel*, 63, 1253, (1984).
11. Wilson, M.A., Pugmire, R.J., Karas, J., Alemany, L.B., Woolfenden, W.R., Grant, D.M., and Given, P.H., *Analytical Chemistry*, 56, 993, (1984).
12. Retcofsky, H.L., *Applied Spectroscopy*, 31, 116, (1977).
13. Durie, R.A., Shewchuk, Y., and Sternhell, S., *Fuel*, 45, 99, (1966).
14. Brown, J.K., Ladner, W.R., and Sheppard, N., *Fuel*, 39, 79, (1960).
15. Brown, J.K., *J. Chem. Soc.*, 744, (1955).
16. Mazumdar, B.K., *Fuel* 43, 78, (1964).
17. Solomon, P.R., Hamblen, D.G., Carangelo, R.M., and Krause, J.L., 19th Symposium (Int.) on Combustion, The Combustion Institute, Pittsburgh, PA, pg. 1139 (1982).
18. Solomon, P.R. and Hamblen, D.G., Finding Order in Coal Pyrolysis Kinetics, Topical Report Submitted to the U.S. Department of Energy, under Contract #DE-AC21-FE05122 (1983).
19. Solomon, P.R. and Hamblen, D.G., Measurement and Theory of Coal Pyrolysis Kinetics in an Entrained Flow Reactor, EPRI Final Report for Project RP 1654-8 (1983).
20. Solomon, P.R., Hamblen, D.G., and Best, P.E., Coal Gasification Reactions with On-Line In-Situ FT-IR/Analysis, DOE Quarterly Reports, Contract #DE-AC21-81FE05122 (1981-1983).
21. Best, P.E., Carangelo, R.M. and Solomon, P.R. ACS Division of Fuel Chem, 29 249 (1984).
22. Solomon, P.R., Serio, M.A., Carangelo, R.M. and Markham, J.R., Very Rapid Pyrolysis, ACS Div. of Fuel Chemistry Preprints, 30 (1985).

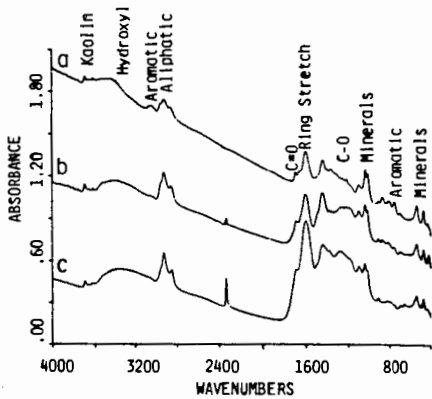


Figure 1. FT-IR Spectra for
 a) a Low Volatile Bituminous Coal,
 b) a High Volatile Bituminous Coal,
 and c) a Lignite.

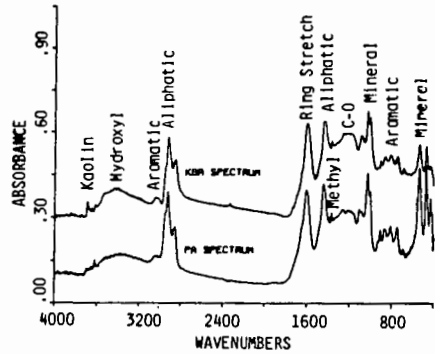


Figure 2. Comparison of KBr Pellet and Photoacoustic Spectra.

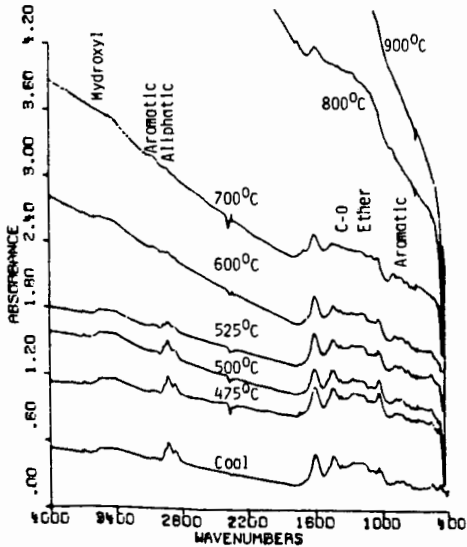


Figure 3. FT-IR Spectra for Chars Produced by Heating at 30°C/min to the Indicated Temperatures.

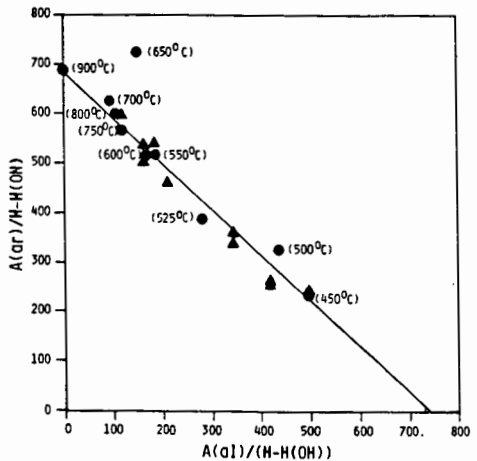


Figure 4. Regression Analysis to Determine Aromatic and Aliphatic Absorptivities for Bituminous Coals, Tars and Chars.

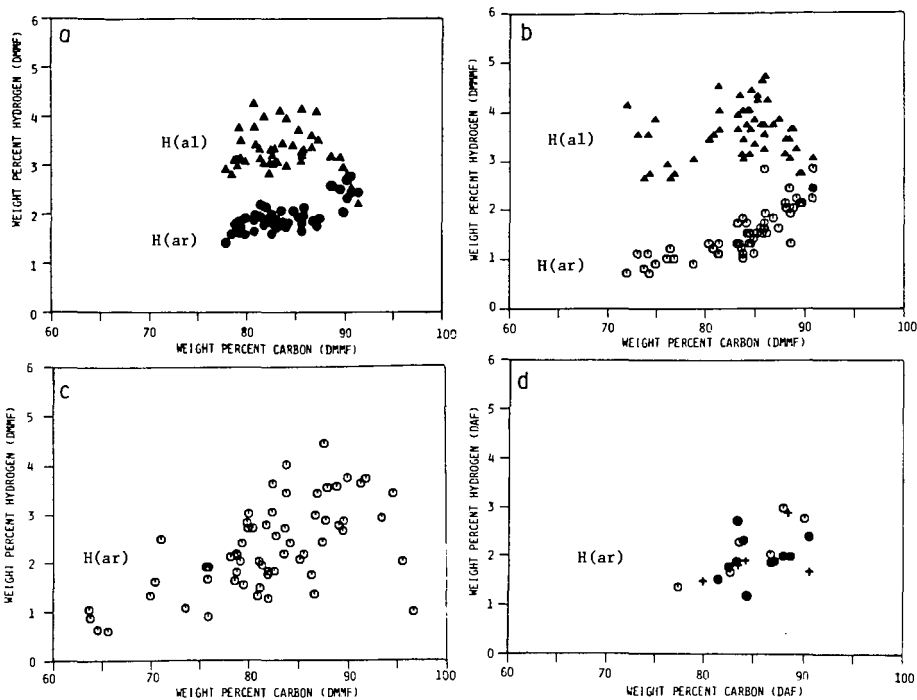


Figure 5. Aliphatic and Aromatic Hydrogen Concentration as a Function of Carbon Concentration. a) FT-IR, Present Results, b) FT-IR (10), c) C^{13} NMR with Dipolar Dephasing (11), and d) Proton NMR (12), (13), + (14).

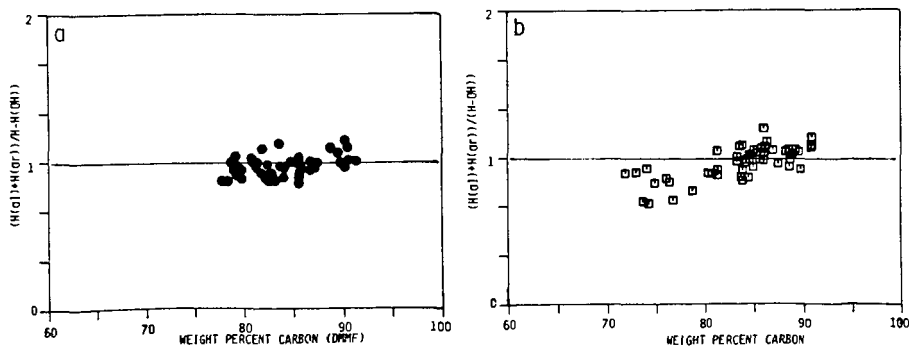


Figure 6. Hydrogen Balance, $(H(al) + H(ar)) / (H - H(OH))$ as a Function of Carbon Concentration a) FT-IR, Present Results and b) FT-IR (10).

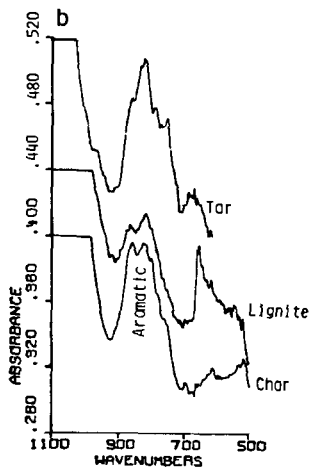
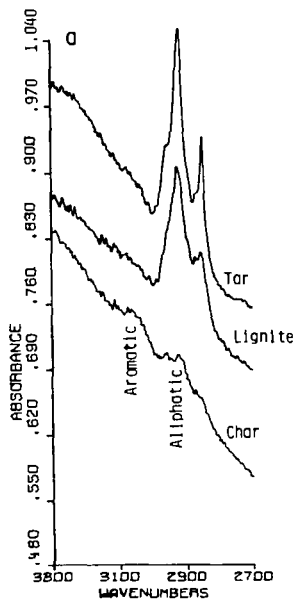


Figure 7. Comparison of Aromatic Hydrogen Stretch at 3100 Wavenumbers and Wag at 800 Wavenumbers.

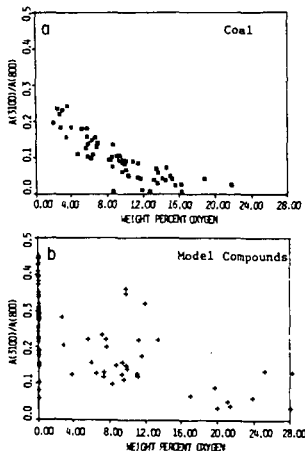


Figure 8. Ratio of Aromatic Stretch (3100 wavenumbers) to Aromatic Wag (800 wavenumbers) Absorption Bands as a Function of Oxygen Concentration.

TABLE I

Author	Ref.	H(al)/H(ar)
Brown	15	0.20
Brown et al.	14	0.33
Reisser et al.	10	0.35
Durie, et al.	13	0.38
Summary of other data		
Retrofsky	12	0.48
Present Results		0.52
Durie, et al.	13	0.56
Mazumdar	16	0.59
Summary of data		
Wilson et al.	11	0.70
Coals and Vitrinites		
Average		0.46

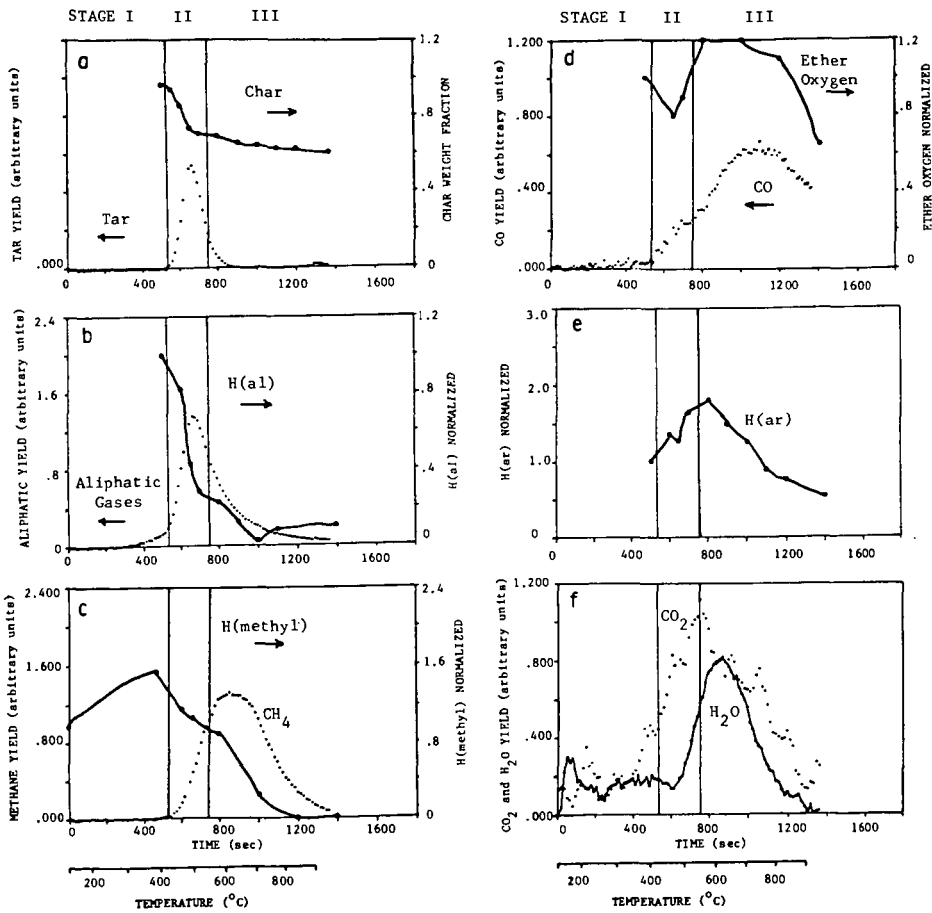


Figure 9. Comparison of Functional Group Composition and Evolved Gases in Slow Pyrolysis.

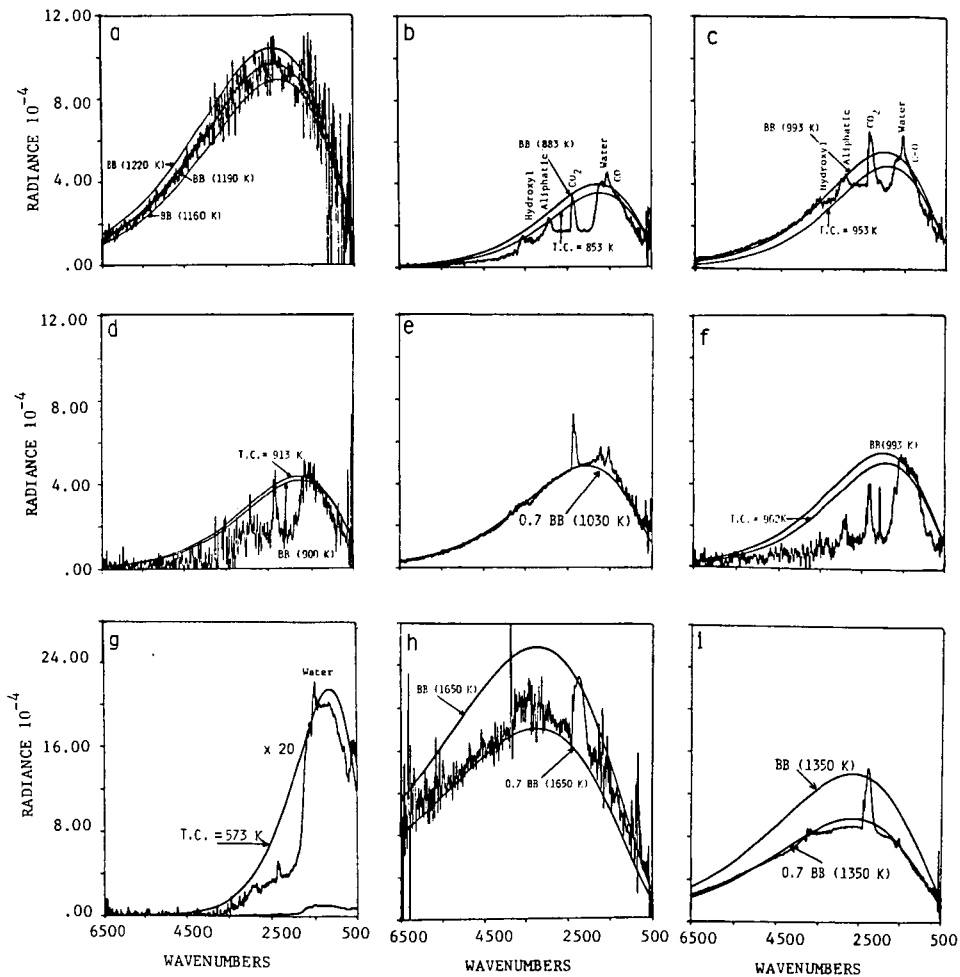


Figure 10. Normalized Emission Spectra for Coal and Char. a) Char in Stage III, b) Coal, c) and d) Char During Stage II, e) Char after Stage III, f) Char During Stage II, g) Coal, h) Lignite Char During Combustion, and i) Bituminous Char During Combustion.